Model and Control of Tractor with Dual Independent Rear Wheel Hydrostatic Transmissions

by

Lucas Garcia

A Report Submitted
to the Faculty of the
Milwaukee School of Engineering
In Partial Fulfillment of the
Requirements for the Degree of
Master of Science in Engineering

Milwaukee, Wisconsin
November 2022

Abstract

The purpose of this paper is to provide a report on a capstone deign project for the Milwaukee School of Engineering's (MSOE) Master of Science in Engineering (MSE) program. The purpose and justification of this project are discussed in detail. The methods and results of this project are reviewed along with relevant published literature. The purpose of this project was to model a tractor with an internal combustion engine (ICE) and dual independent rear wheel hydrostatic transmission (HST). This modeling, control, and analysis were performed with MATLAB and Simulink. The control algorithm was loaded into a physical tractor that is currently housed at the MSOE Fluid Power Institute (FPI), and experimental data were compared to simulation results. This project is intended as a first step to model the complete tractor system and to provide basic speed control, so that future MSOE, or FPI, projects may add additional advanced features, such as semi-autonomous or fully autonomous controls, possibly with Radio Detection and Ranging (RADAR) or Light Detection and Ranging (LiDAR) sensors. The primary goal of the simulation was to produce stable results of hydraulic and mechanical states under normal operator conditions.

Table of Contents

List of Figures

Nomenclature

Symbols

a – Acceleration

b_{eff} – Effective Damping Coefficient

C – Leakage Coefficient

F_t – Tractive Force

J_m – Moment of Inertia of Hydraulic Motor and Wheel

kv – Flow Coefficient of Valve

M_{eff} – Effective Mass

m – Mass

P – Pressure

Q – Volumetric Flow Rate

r_w – Wheel Radius

T – Torque

T_L – Torque Load on Motor Shaft

V – Volume

v – Velocity

V_i - Theoretical Displacement of a Pump or Motor

V_m - Displacement of a Motor

V_{ip} – Maximum Displacement of a Pump

x – Horizontal Position

y – Vertical Position

β – Bulk Modulus of Oil

Δ – Change in Value

ε – Angle of Swash Plate

θ – Rotational Position

μ - Dynamic Viscosity

ρ – Density of Oil

ω – Rotational Speed

Abbreviations

ASABE – American Society of Agricultural and Biological Engineers

DEC - Decimal

FPI – Fluid Power Institute

GPM – Gallons per Minute

HST – Hydrostatic Transmission

ICE – Internal Combustion Engine

IN – Inch

LBS - Pounds

MPH – Miles per Hour

MSE – Master of Science in Engineering

MSOE – Milwaukee School of Engineering

PSI – Pressure per Square Inch

RPM – Revolutions per Minute

SC – Signal Conditioner

VCU – Vehicle Controller Unit

Introduction

A hydrostatic transmission exists any time a hydraulic pump is connected, and dedicated, to providing flow to one, or more, hydraulic motors. These transmissions can be used to prevent lugging on the prime mover -- for example, an Internal Combustion Engine (ICE) -- because of their ability to adjust pump and/or motor displacements. This configuration can result in a “constant output power” mode [1]. Figure 1 shows the main components of a hydrostatic system, the pump on the left-hand side and the motor on the-right hand side.

Figure 1: Hydrostatic Pump and Motor [2].

There is a combination of different setups with hydrostatic systems with regard to how the hydraulic motor is connected to the wheel(s) of the off-highway equipment. For example, a wheel loader may have a hydraulic motor drive a driveshaft that uses a differential transmission to provide power transmission to the rear wheels. In cases where a mechanical solution, such as a differential gear box, is not being implemented for rear

wheel vehicle drive, those features need to be included in the electronic control of the hydraulic motors.

Figure 2 shows a single pump, dual motor tractor HST. A drive shaft, gear box, or wheel could be connected directly to the motor shaft depending on the specifications needed for the vehicle.

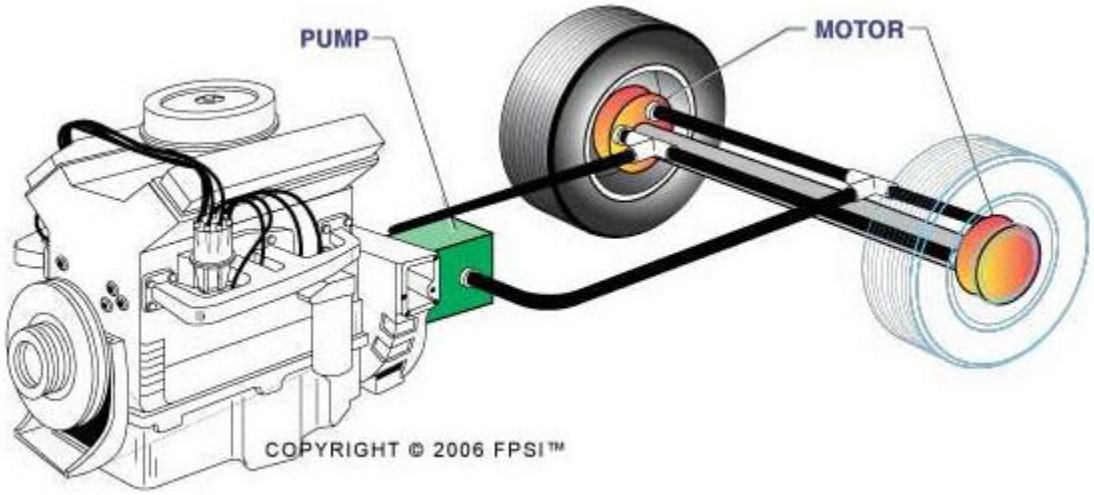

Figure 2: Example of HST in Tractor [3].

In cases where there is more than one hydrostatic system, with more than one connected set of wheels, control schemes are needed to ensure there are not adverse effects from wheels slipping. In applications such as forestry trucks, mechanical brakes are used with a combination of sensors and an electronic controller to prevent wheel slip [4]. In cases where mechanical brakes are not very useful, the wheel anti-slip and/or traction control would need to be handled entirely by the hydraulic controls.

Figure 2 shows a case where an ICE is driving a single pump, which supplies flow to dual motors, directly connected to wheels. This simple illustration is an example of a system which would require a solution for situations like turning, or slippery terrain, that

may cause the wheel to slip or loose traction. This system also requires a solution for controlling the total power consumed by the HST, such that it is not greater than the power provided by the ICE.

The systems needed to create a HST include the hydraulic motor, hydraulic pump, hydraulic hoses and fittings, electronic sensors and actuators, and an electronic control unit. All of these systems must be designed with parts that are compatible with each other, as well as capable of performing the physical needs of the vehicle they are placed on. Only once a system meets all of these hardware requirements can one, or many, control systems be designed and implemented on a vehicle with an HST.

Figure 1 shows two hoses connecting the pump and motor. These hoses, or lines, are typically given a reference name in the hydraulic schematics. The current schematics of this HST does not designate a name for these two lines. For the purposes of this project, the HST line connected to the inlet, or port A, of the motor will be referred to as line A. The line connected to the outlet, or port B, of the motor will be referred to as line B.

In this project, a ¼-scale tractor with dual independent rear wheel HSTs was modeled and controlled via a Vehicle Control Unit (VCU). This tractor was designed by previous MSOE undergraduate engineering senior design teams to compete in the American Society of Agricultural and Biological Engineers (ASABE) ¼-scale tractor pull competition. This tractor contains two independent hydrostatic systems along with a working engine and frame that was designed with the constraints of ASABE's tractor pull competition in mind.

Each hydraulic motor is connected to a rear wheel. This means that part of the control scheme has to consider the speed of the rear wheels relative to each other. The previous teams electrical and hydraulic schematics are maintained by FPI. The previous MSOE senior design teams' documentation did not include software specific control schemes. The previous VCU manufacturer's website claims it is compatible with MATLAB and Simulink [5]. However, there were several issues attempting to connect to this VCU with the manufacturer's software. Therefore, the decision to acquire a new VCU for installation on the tractor was made.

Husco Inc. has provided the new VCU that has been installed on the tractor. This VCU is programmable with respect to the Simulink environment. This is a key feature required for this project as it allows Simulink models of vehicle system dynamics to be tested with the VCU control software very quickly and easily. The Simulink model for this project takes input from two virtual sensors, the steering wheel and accelerator pedal. The model provides several outputs, all relating to the kinematic and dynamic states of the vehicle. This model uses open loop speed control as the control scheme.

Based on the previous electrical and hydraulic schematics of the tractor, it was determined that an additional signal conditioner (SC) needed to be purchased to allow the VCU to sense the speed of the engine. This part was not installed on the vehicle due to time restraints and did not affect the results gathered for this project. For optimal performance of the tractor, it is recommended that future MSOE teams install this sensor and integrate the engine speed into the control scheme.

The second part of this project focused on the physical installation and testing of this hardware and control scheme, as well as the validation of the Simulink model. It is intended that this tractor will be used by future FPI students to explore further advanced automation processes, and to assist with future projects for undergraduates and graduates alike.

A solid physics-based simulation and control scheme set in a MATLAB framework is sometimes too advanced for undergraduate student groups or takes too much time to implement. Giving MSOE and FPI students these tools by way of this capstone project can help make automation and controls projects in the future more advanced and fun for students new to real-world automation. This project takes advanced graduate level simulation and control concepts and places them in an environment that is easy to understand and use by less experienced engineering students.

FPI's Advanced Technologies Department is eager to assist students who would like to learn and implement automation, such as LiDAR and RADAR assisted autonomous vehicles [6]. Students who are interested in more advanced control schemes with advanced sensors can use this tractor to perform specific functions in an efficient way. The need for a physical vehicle, such as this tractor, using hydraulic transmissions, where students can work with experimental software in a real-world scenario is a justifiable reason for this capstone project.

Background

Analytical models and simulations for positive displacement hydraulic pumps and motors have long been established, with regards to the theoretical hydraulic flow,

rotational speed, positive volume displacement, and shaft torque [7]. Wilson [7] gives the ideal theoretical volumetric oil flow in Equation (1) and shaft torque in Equation (2) of a pump or motor. Thus,

$$Q = \omega \varepsilon V_i \ , \tag{1}$$

$$T = \Delta P \varepsilon V_i \, . \tag{2}$$

There are several torque and flow loss terms that can be added to the flow and torque terms, depending on the impact of each physical loss that term is expressing. These terms are best applied to models based on results from experimental data [8]. For the purposes of this project, these pumps and motors are considered ideal.

Egeland and Gravdahl [9] describe the pressure of a HST line, where V is the lumped volume of the hydraulic line, and C is the leakage coefficient of the line as Equation (3) and Equation (4), where P_A is the pressure in line A and P_B is the pressure in line B. Thus,

$$\frac{V}{\beta} \dot{P}_A = -V_m \omega_m + \varepsilon V_{ip} \omega_p - C P_A , \tag{3}$$

$$\frac{V}{\beta} \dot{P}_B = V_m \omega_m - \varepsilon V_{ip} \omega_p - C P_B \, . \tag{4}$$

Egeland and Gravdahl's [9] calculation of the HST line pressure uses one term to lump all leakages of a hydrostatic system into one term. The leakage flow from a transmission line come from different sources and can be broken down into their component parts. The different valves used in HST account for some of this leakage flow. There are three different types of valves in the HST that contribute flow to the line

volume: check valve flow, Q_c, relief valve flow, Q_{RFV}, and flushing valve flow, Q_F [10]. Check valves are used on each transmission line to allow oil to enter the transmission line if the line pressure becomes lower than the charge pump relief valve setting, P_C. Equation (5) shows this flow, often referred to as make up oil [11]. There is one relief valve per transmission line to ensure line pressure does not exceed a specified maximum pressure. Equation (6) shows if the pressure in the transmission line is higher than the cracking pressure of the relief valve, P_{RFV}, oil will flow out of the line and into tank [11]. This maximum pressure is chosen based on the maximum pressure rating of the components in the HST [10]. Thus,

$$Q_c = kv_c\sqrt{P_C - P} \qquad \text{when } P_C\text{-}P > 0, \tag{5}$$

$$Q_{RFV} = kv_{RFV}\sqrt{P - P_{tank}} \qquad \text{when } P\text{-}P_{RFV} > 0. \tag{6}$$

The flushing valve is a three-port, three-position valve that is designed to have a nearly constant amount of oil flow from the transmission line to the tank. This is needed to ensure the hydraulic oil in the transmission lines is sent through the cooling and filtration system. The flushing valve will allow flow from the transmission line with the lower pressure to flow to tank. This flushing valve is modeled as an open center valve, meaning if the two HST line pressures are nearly equal, flow from both transmission lines will flow to tank [11]. Equation (7) and Equation (8) describe the flow out of the HST line based on the pressure of both lines [11]. Thus,

$$Q_{FA} = kv_F\sqrt{P_A - P_{tank}} \qquad \text{when } P_B\text{-}P_A \geq 0, \tag{7}$$

$$Q_{FB} = kv_F\sqrt{P_B - P_{tank}} \qquad \text{when } P_A\text{-}P_B \geq 0. \tag{8}$$

Substituting the flows from the valves in a HST into Equation (3), the pressure in each line can be expressed [11] by Equation (9) and Equation (10). Thus,

$$\frac{V}{\beta}\dot{P}_A = -V_m\omega_m + \varepsilon V_{ip}\omega_p - Q_{FA} - Q_{RFV} + Q_C - CP_A, \tag{9}$$

$$\frac{V}{\beta}\dot{P}_B = V_m\omega_m - \varepsilon V_{ip}\omega_p - Q_{FB} - Q_{RFV} + Q_C - CP_B. \tag{10}$$

Equation (11) and Equation (12) models vehicle dynamics, where a_t is the wheel's translational acceleration, M_{eff} is the effective mass of the vehicle, b_{eff} is the effective damping and the only force acting on the vehicle is the traction force, F_T, of the tractor [12]. The effective mass, Equation (13), involves transforming the hydraulic motor's inertia, J_m, by the inverse squared wheel radius, r_w, and summing the mass of the tractor, m_t [12]. There are two wheels and therefore the effective mass that each wheel accelerates is half of the total tractor mass. Thus,

$$F_t = M_{eff}a_t + b_{eff}v_t, \tag{11}$$

$$\dot{v}_t = a_t, \tag{12}$$

$$M_{eff} = \frac{m_t}{2} + J_m\left(\frac{1}{r_W{}^2}\right). \tag{13}$$

Equation (14) and Equation (15) describe the transformation of traction force and tractor velocity to wheel torque load and wheel speed, respectively [12]. The hydraulic motor is directly coupled to the wheel, thereby making the wheel speed and wheel torque equal to the motor speed and motor torque, respectively. Thus,

$$F_t = \frac{T_L}{r_W}, \tag{14}$$

$$\omega_W = \frac{v_t}{r_W}. \tag{15}$$

To model the kinematics of the tractor, using the approach by Dudek and Jenkin [13] for a differential drive robot is applicable in this application. Using the velocity of the right wheel, v_r, and left wheel, v_l, with the distance between the two wheels, L, the heading of the tractor, θ, can be described as Equation (16). Equation (17) and Equation (18) describe the position of the tractor in a two-dimensional plane on an x and y axis. Thus,

$$\theta = \frac{1}{L}\int v_r - v_l, \tag{16}$$

$$x = \frac{1}{2}\int (v_r + v_l)\cos\theta, \tag{17}$$

$$y = \frac{1}{2}\int (v_r + v_l)\sin\theta. \tag{18}$$

There are several different methodologies for modeling engine behavior. These methods are often combined with empirical descriptions to aid in the speed and simplicity of modeling ICEs that interact with other systems [14]. The engine behavior is not a focus for this project, and therefore, a grey box method was used. Empirical engine data recorded by previous FPI employees at full engine throttle will be used to describe the speed of the engine given an applied torque load. There was also a first order transfer function applied to the speed output of this grey box engine model to account for fuel lag

and engine dynamics. The time constant for this lag was estimated by previous FPI employees while performance testing this engine.

The schematic shown in Figure 3 was created by FPI employees for this project and represents the tractor's hydraulic system in 2022.

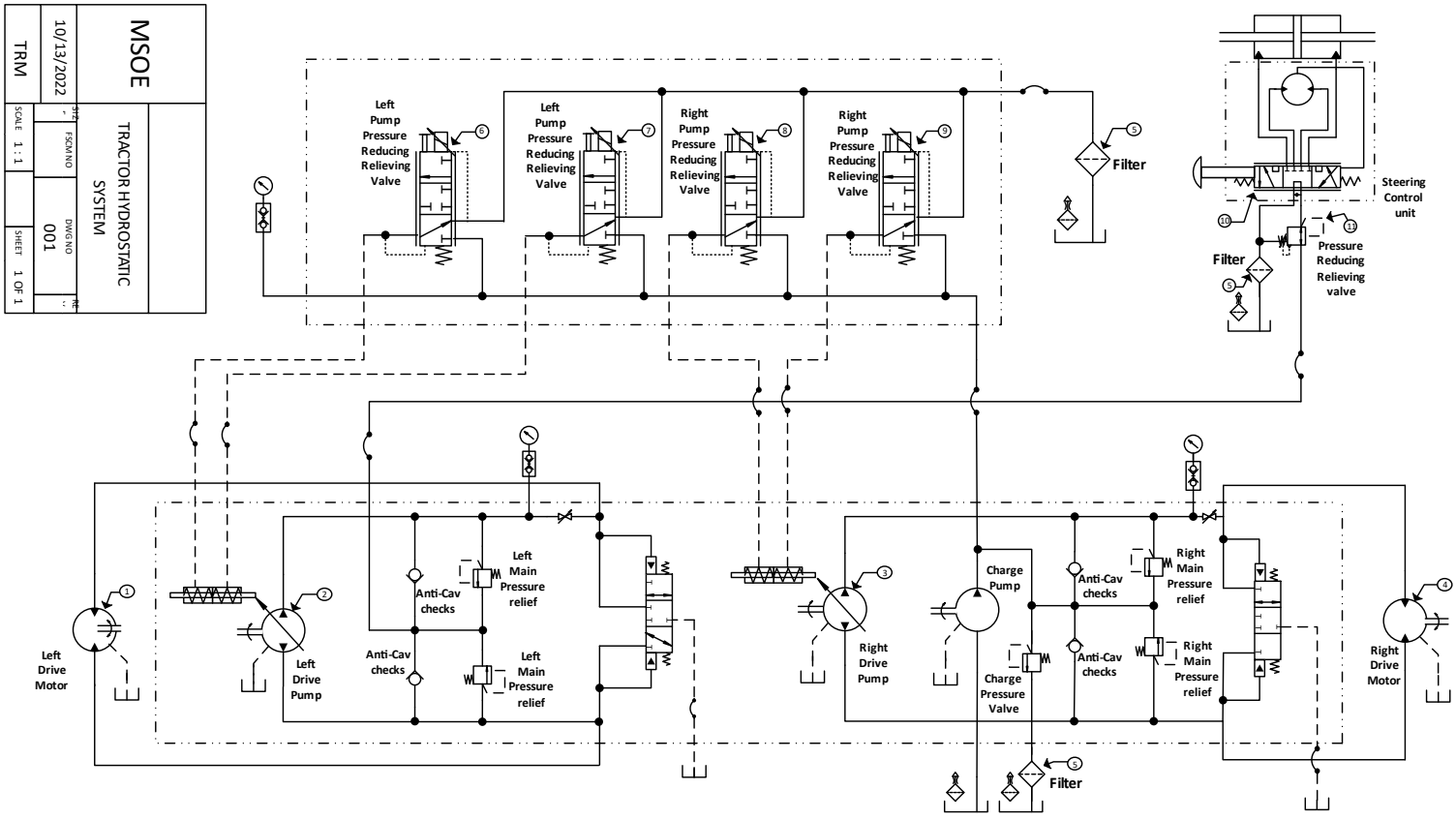

Figure 3: HST Hydraulic System Schematic for Project Tractor, Dated 2022.

The HST includes two tandem Poclain Hydraulics PM-10 variable displacement pumps (shown in Figure 4), which are each individually connected with two Eaton 2000 series hydraulic motors (shown in Figure 5).

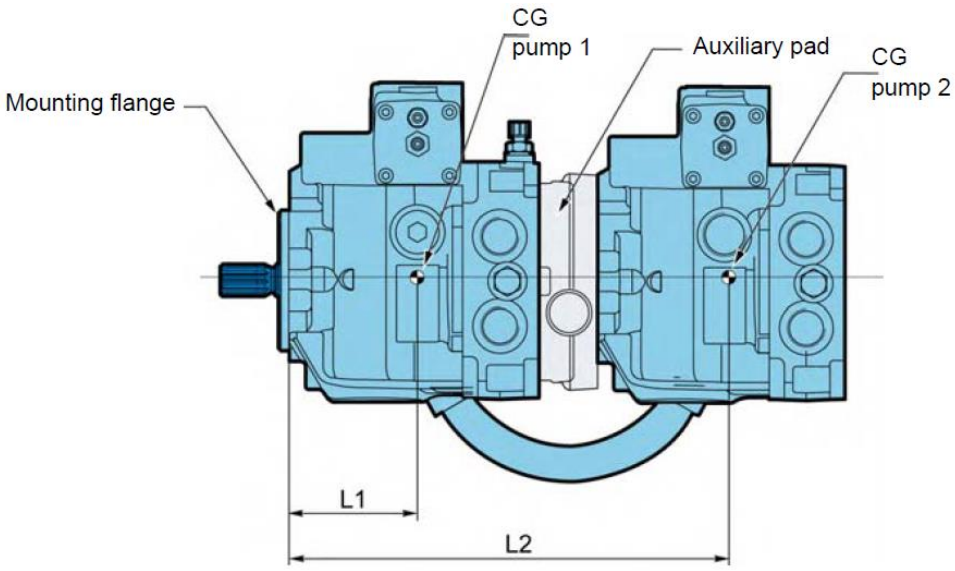

Figure 4: Poclain PM-10 Tandem Pumps [15].

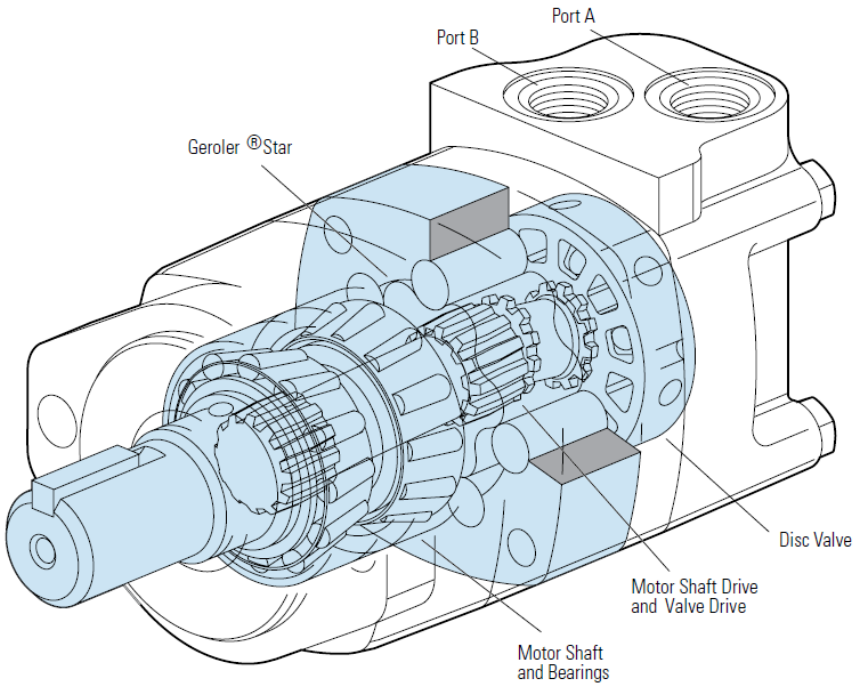

Figure 5: Eaton 2000 Hydraulic Motor [16].

This tractor has a 31-HP Vanguard Briggs and Stratton gasoline-powered ICE, model series 290000. The ICE is equipped with a governor that is factory set to 3600 RPM maximum speed and an adjustable idle governor [10]. The tractor's original design

included an electronically controlled engine throttle. This part was removed and replaced with a manual engine throttle lever due to the incompatibility of the electric throttle and the new VCU's specifications.

The vehicle was previously built to satisfy the ASABE ¼-scale tractor pull competition rules. Those sets of specifications will no longer be required, as this tractor is to be used only for projects involving FPI employees and MSOE students. Any item not mentioned in this report was previously selected by the 2017 MSOE tractor team.

Review of Literature

There have been many books and papers written about the modeling of hydraulic pumps and motors, the first notable author being Wilson in 1950 [7]. There was improvement to HST modeling made by Merritt in the 1960s [17]. This work was further improved and updated by Manring in the 2000s [18]. These improvements in HST modeling focused mainly on theoretical issues. These sources contain relevant information including mathematical models for the basic features found in an HST.

Work focused on HST used in a laboratory environment to simulate physical machine hardware setups was the focus of thesis work by Lennevi [19] at Linköping University and Prasetiawan *et al.* [20] at the University of Illinois. In both the laboratory setups at Linköping University and the University of Illinois, the prime movers were electric motors. Hydraulic valves were used to simulate different loads. This work is relevant to this capstone project but lacks the inclusion of an ICE as a prime move and the inclusion of vehicle dynamics in the simulation and validation testing of the load.

The development of Simulink models of hydrostatic systems was documented in an article by Jedrzykiewicz *et al.* [21]. This article includes many different sub-systems of an HST, including an ICE as the prime mover. The Simulink models in this article do not account for an electronic controller.

Nevala *et al.* [4] and Carlsson [22] at Linköping University have both done work developing control schemes for HST in forestry vehicles. Work done by Nevala *et al* [4]. focused on fuzzy logic control to minimize slip and did not model an HST. Carlsson developed a MATLAB/Simulink model for the hydraulic transmission line pressure of Komatsu forestry vehicles.

Many of these previous works include relevant and similar work that was conducted with this capstone project. Previous work from Carlsson [22], Jedrzykiewicz *et al.* [21], and Lennevi [19] are most relevant to this project. They lack, however, the inclusion of modeling of an independent, dual rear wheel off-highway vehicle powered by an ICE and controlled by a VCU. They also do not discuss the integration of Simulink models and VCU programming for purposes of experimental test data to verify Simulink models.

Simulation Methods

A Simulink model of the entire tractor system was created using several sub-systems for organizational purposes. The organizational flow of the model was constructed such that system and sub-system inputs are on the left-hand side of the model space and outputs to said systems are on the right-hand side of the model space. This is evident in the model's top view. Figure 6 shows the system inputs, steering angle and

foot pedal command, on the left. System outputs, tractor kinematic information, are shown on the right.

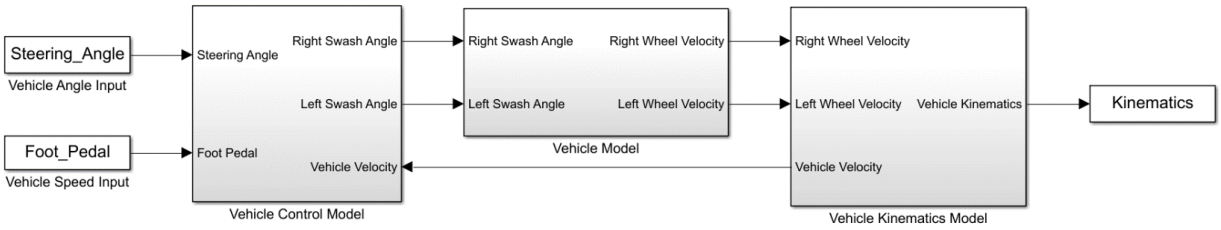

Figure 6: Simulink Model, Top View.

The vehicle control sub-model is responsible for controlling the speed of the tractor's rear wheels. This model is not the focus of this paper and currently contains a very basic open loop speed control. This sub-model contains the information that was downloaded into the VCU to control the physical tractor. For a complete view of this, and any other sub-model not shown in this section, please reference Appendix A.

Sub-systems that exchange information are organized such that physical inputs and outputs are shown parallel to each other to emphasize the energy exchange occurring between systems. An example of this can be seen in Figure 7. The information exchanged between the right hydrostat model and the right dynamics model is motor speed and torque, which together describe the energy flow between the two models. These organizational decisions are intended to make the model more clear to users of the model by using consistent rules with regard to model organization [23].

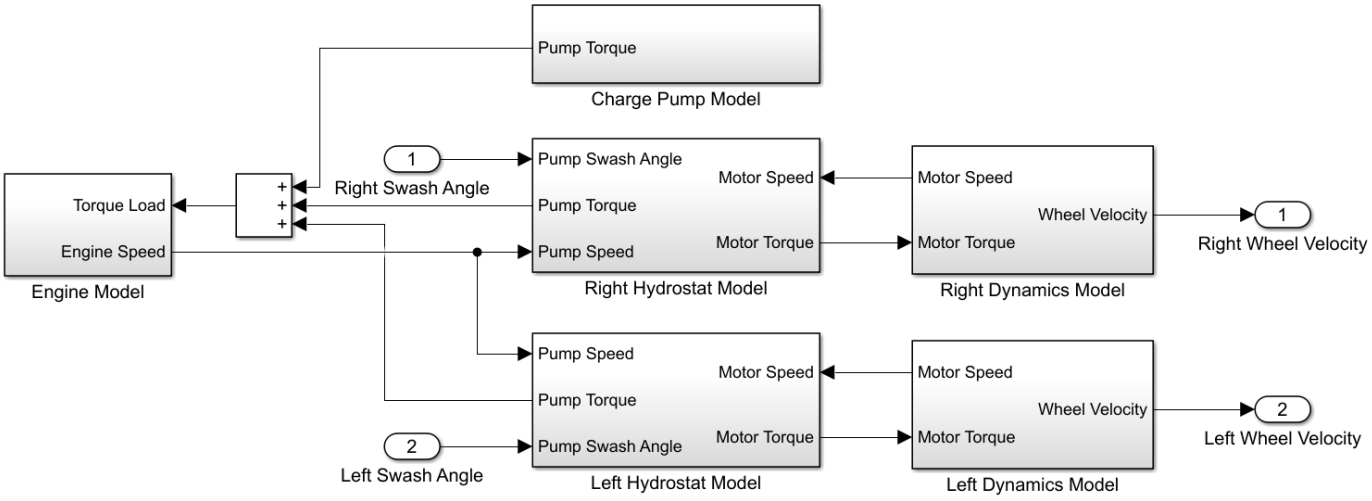

Figure 7: Vehicle Sub-Model.

The vehicle sub-model can be broken down into three distinct groups: ICE, hydraulic, and mechanical. The ICE Model contains a single dimensional look up table that contains empirical data of the engine at 100% engine throttle. The ICE model also has a first order transfer function to account for fuel lag and other engine dynamic responses, seen in Figure 8. This Simulink schema, along with many of the hydraulic Simulink schemas, was used by Williams at MSOE [24].

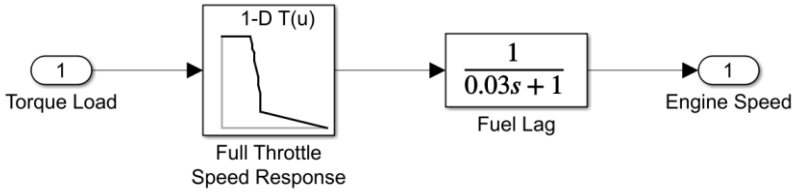

Figure 8: Engine Sub-Model.

The hydraulic sub-models include the left and right hydrostat sub-models and the charge pump sub-model. The charge pump sub-model only contains a pump torque model, see Appendix A. The right and left hydrostat sub-models are identical, and only the left side is shown in this section. The left hydrostat model is arranged to resemble the

hydraulic schematic. Each valve is shown in line with its transmission line.

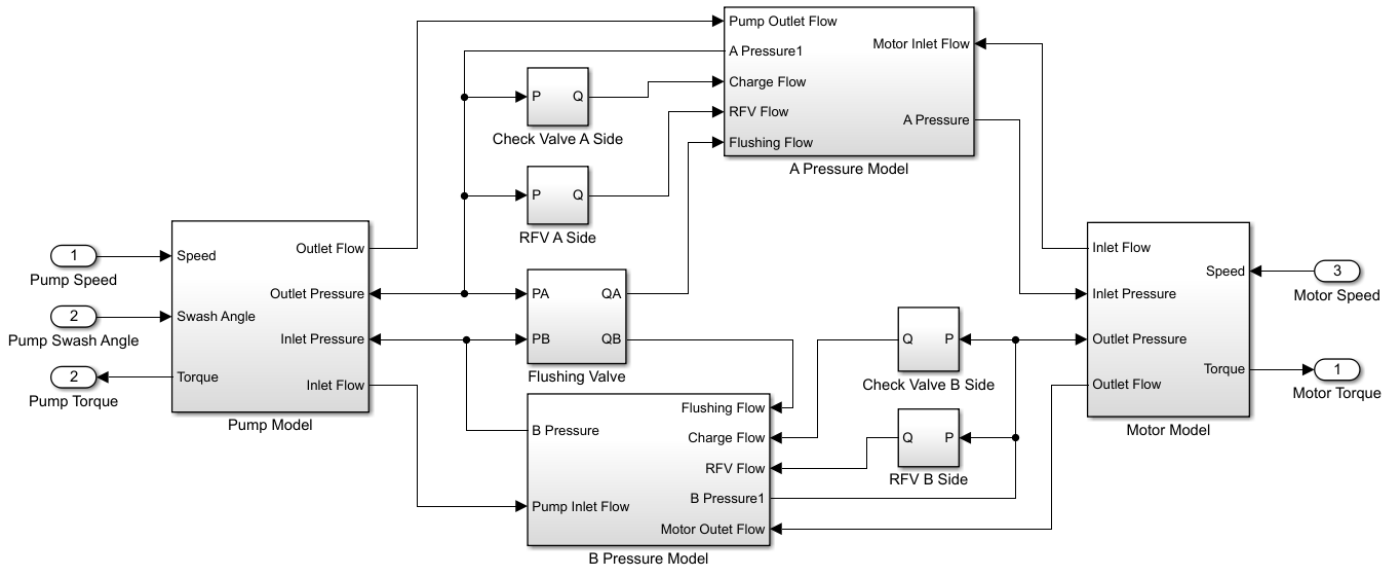

Figure 9: Left Hydrostat Sub-Model.

The A and B side pressure models contain the six flows described in Equation (9) with an additional saturation block to ensure no flow is allowed in the event of a negative pressure [24].

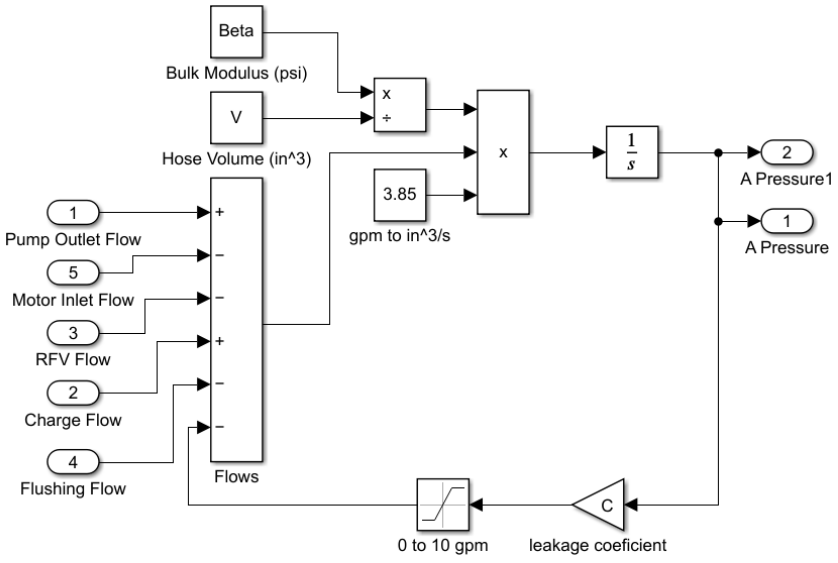

Figure 10: Pressure A Sub-Model.

The pump and motor models contain Equation (1) and Equation (2) in the flow and torque model, respectively. These represent the ideal flow and torque of a motor and do not include mechanical or volumetric inefficiencies, seen in Figure 11 and Figure 12.

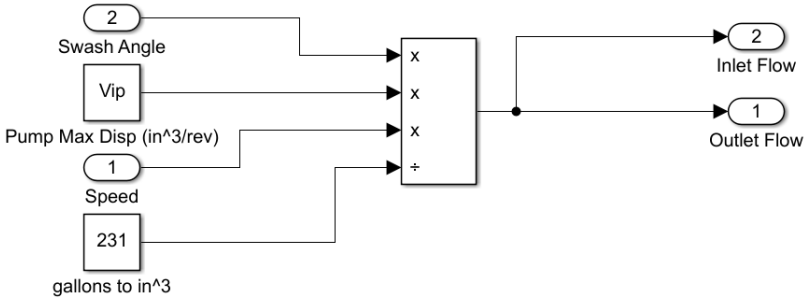

Figure 11: Pump Flow Sub-Model.

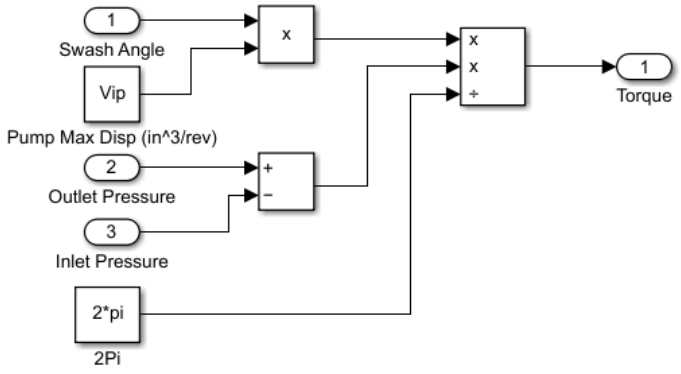

Figure 12: Pump Torque Sub-Model.

The vehicle dynamic sub-model contains the wheel sub-model that implements Equation (14) and Equation (15). Figure 13 shows an external load sub-model; however, it is not currently used and is a place holder for future research. Figure 14 shows the vehicle dynamics sub-model. The vehicle sub-model uses techniques from Williams [24].

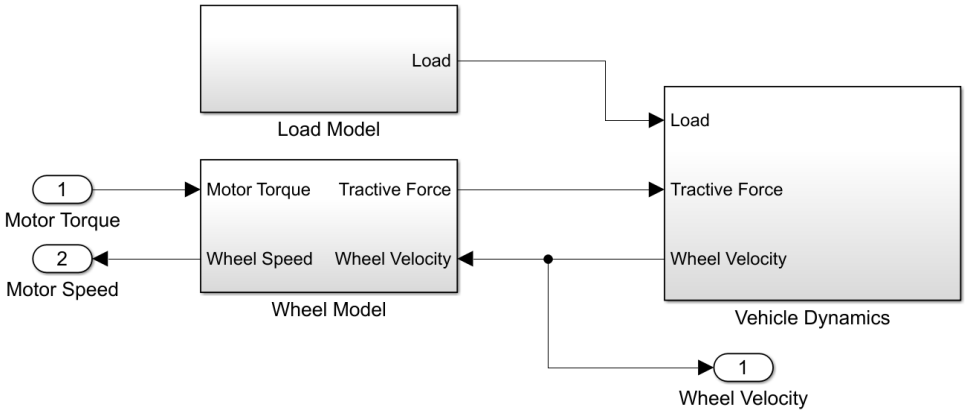

Figure 13: Vehicle Sub-Model.

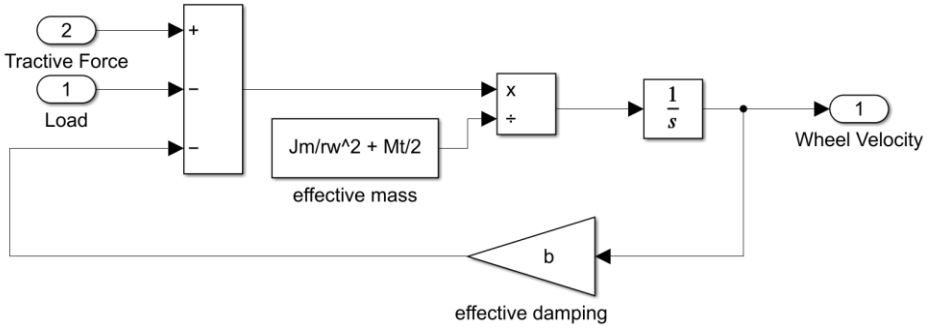

Figure 14: Vehicle Dynamics Sub-Model.

The final sub-model from

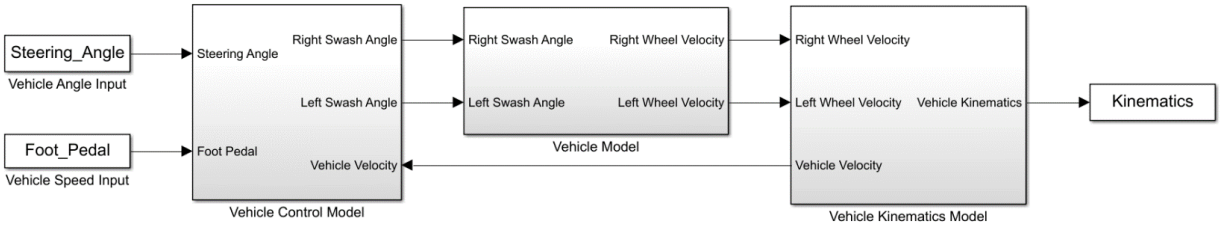

Figure 6 is the vehicle kinematics model. This model implements Equation (16), Equation (17), and Equation (18) to produce seven different terms to describe the motion of the tractor and its wheels. These terms will be used for future control schemes or future analyses.

This model features some assumptions. These include assuming constant oil bulk modulus and oil density despite real-world temperature and pressure changes on the oil. There are simplifications for valve characteristics. There are simplifications made for pump and motor inefficiencies. It is assumed the tank pressure is zero psi. The engine throttle is not adjustable and is always set to 100% throttle. HST relief valves and check valves flow to tank in the model, while the actual valves flow to the make-up oil lines.

Simulation Results

Two simulation runs were initially conducted for verification purposes. The simulation needed to verify the model was stable and produced results that were within an expected range. Specifically, the HST pressures, HST flows, and vehicle speed were evaluated. The difference between the two runs was the weight of the vehicle. The first run had a vehicle weight of 800 lbs, while the second run had a vehicle weight of 100 lbs. The 800 lb simulation was chosen to ensure that the simulated relief valve behavior is correct. If the torque load on a motor is relatively large, then the pressure in the transmission lines will increase until they reach the relief cracking pressure, and flow should be allowed to tank, thus relieving transmission line pressure. These relief valves ensure line pressures stay within the pressure ratings of all hydraulic components. The 100 lb simulation was chosen because the relief valves should not be in operation with a vehicle weight this small.

These analyses were run with the steering wheel at 0 degrees, meaning the vehicle will drive straight ahead. The right and left HST and wheels then behave identically. Because of this steering input, some of the kinematic information will not be verified

since the vehicle was traveling in a straight line, with the left and right wheels behaving the same way. The vehicle's heading and rotational speed is zero for all simulations. Therefore, only the left side of the tractor is analyzed in this section.

The two simulation runs had the same foot pedal step up and step down inputs. Comparing the commanded foot pedal inputs, the swash command and vehicle speed in Figure 15 show the tractor velocity follows the swash command very closely with a tractor weight of 0 lbs. There is a rate limiter in the swash command to limit the command rise rate to full range in 1 second and to limit the fall rate to full range in 3 seconds.

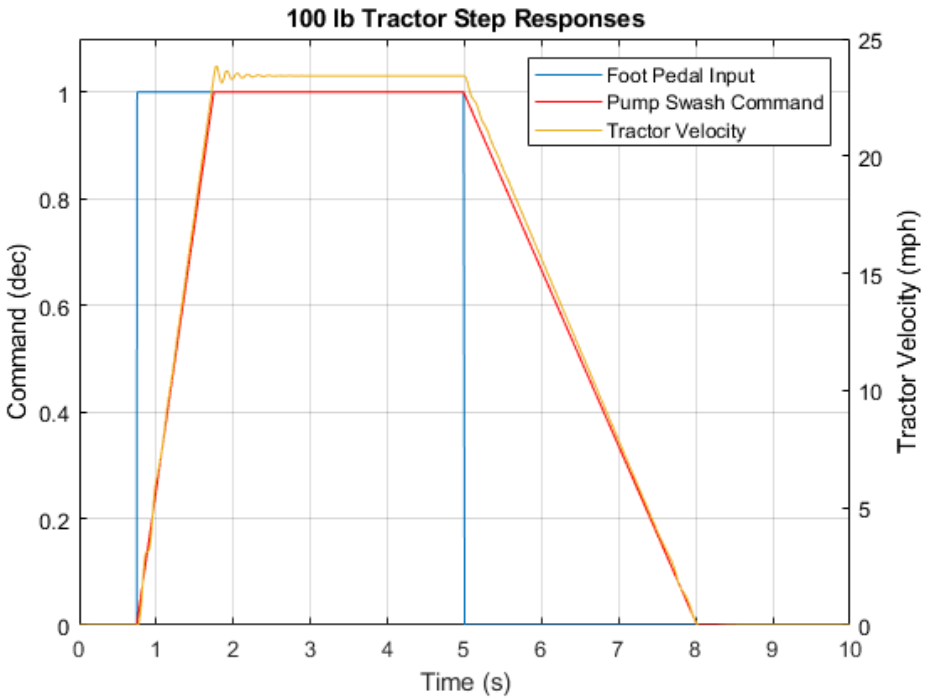

Figure 15: Step Response of 100 lb Tractor.

Figure 16 shows a difference in tractor acceleration when the weight is increased. While there is a relatively small difference in the vehicle speed response with an increase in vehicle weight, a large difference in the transmission line pressures can be seen in

Figure 17, due to the added torque needed to get the heavier vehicle up to speed in the same amount of time.

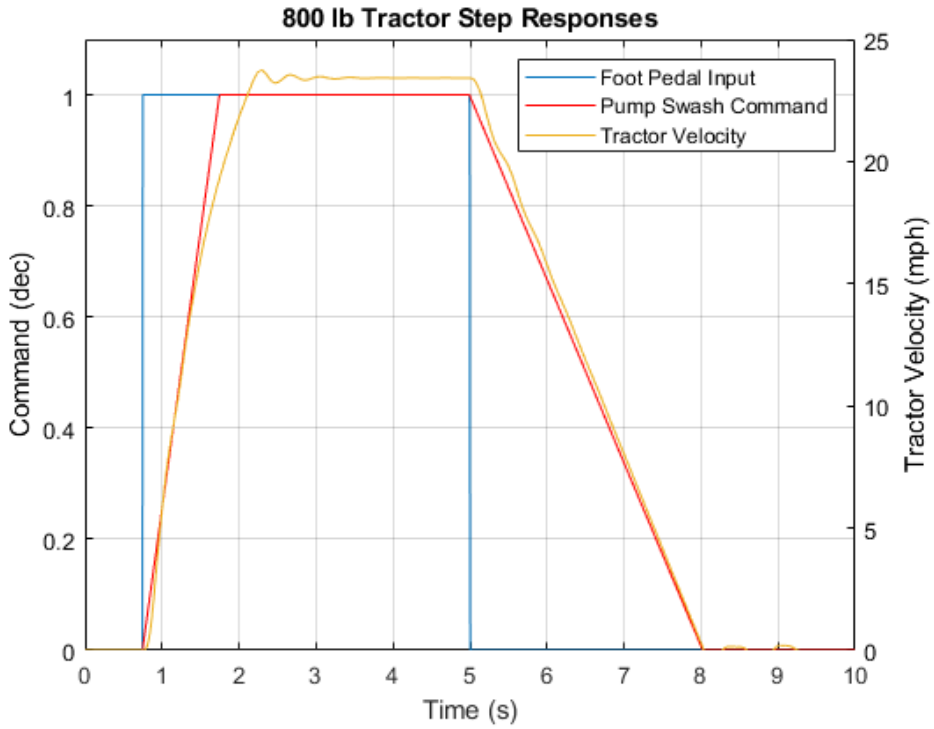

Figure 16: Step Response of 800 lb Tractor.

Figure 17 shows the HST line A pressure reaching above the cracking pressure, 4100 psi, of the relief valve. This means there should be flow through the A relief valve to tank, whereas with the 100 lb tractor there would be no flow. This can be seen in Figure 18. Figure 18 also shows the flows from the three valves in each transmission line. All flows are shown as positive values; however, the direction of flow for the flushing and relief valve is out of the HST line and the direction of flow for the check valve is into the HST line.

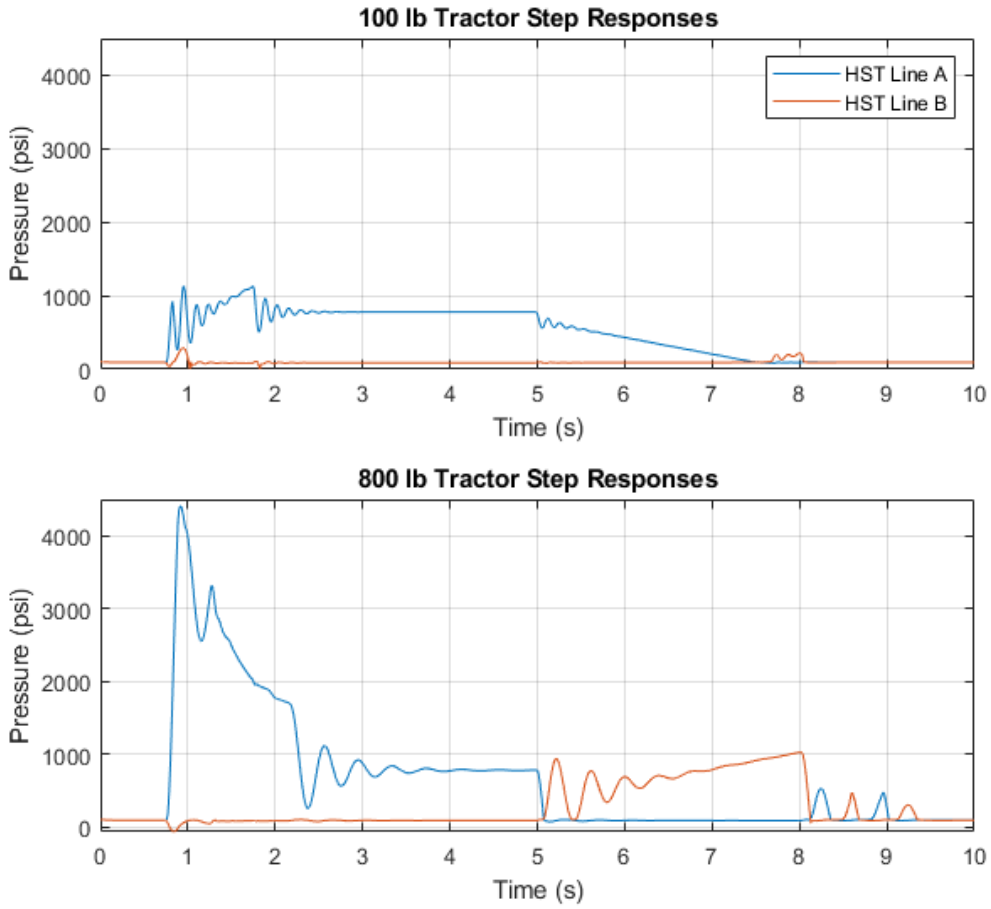

Figure 17: HST Line Pressures During Step Inputs.

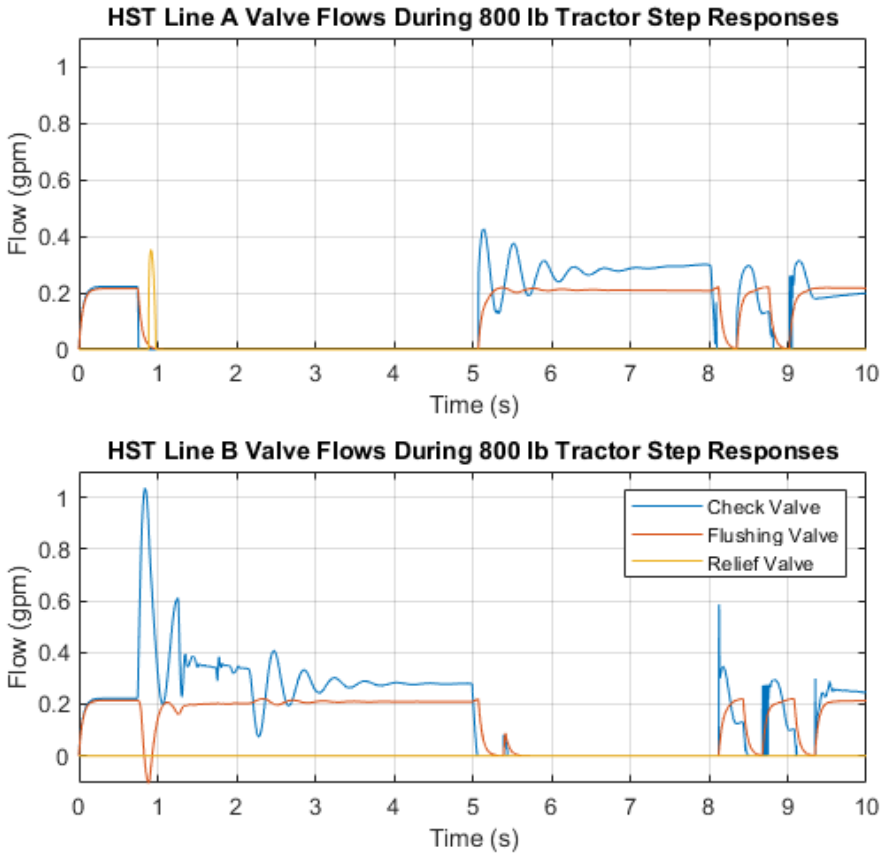

Figure 18: HST Valve Flows for 800 lb Tractor Step Responses.

The increase in transmission pressure, results in an increase of torque needed from the pump to accelerate the heavier tractor. This is provided from the engine. When the torque load exceeds a certain value, the engine speed will decrease. This can be seen in Figure 19. This engine speed decrease occurs in the 800 lb machine and not in the 100 lb machine, because the engine can stay at full speed while delivering the torque needed to accelerate the lighter tractor.

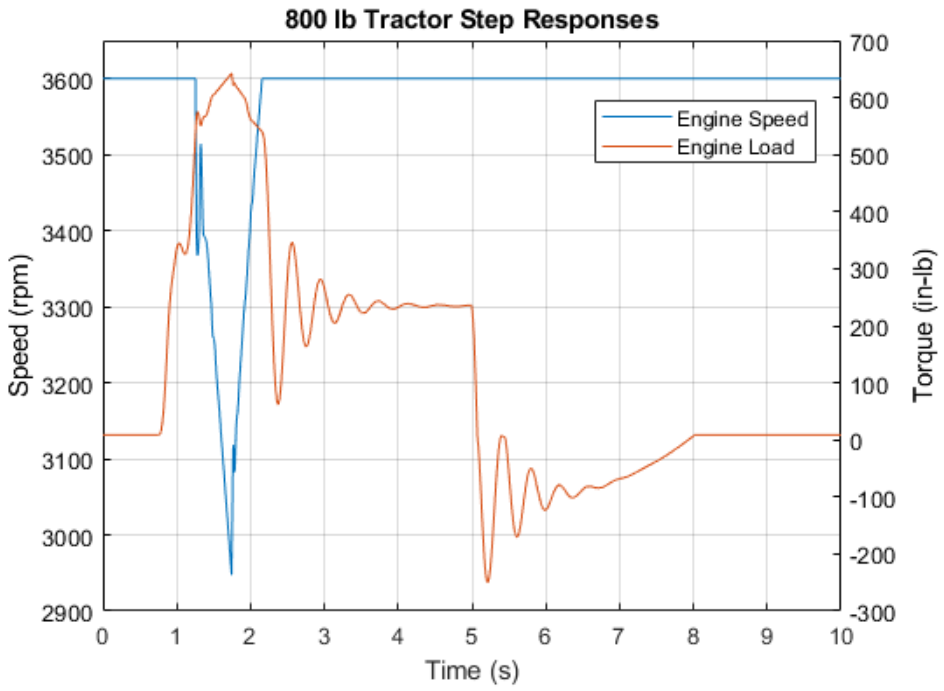

Figure 19: Engine Speed and Torque During 800 lb Tractor Step Input.

Experimental Methods

Experimental tests were required to verify both the accuracy of the Simulink model, as well as the control scheme in the VCU. The experimental tests can offer more insight into the actual properties of the components of the tractor. The tractor used in this project required many repairs and upgrades to mechanical and electrical items. The amount of time and resources needed to bring the tractor into an operable condition was greater than initially estimated at the start of this project.

This project's experimental testing required a human to operate a hydraulic vehicle. The largest safety concerns exist for the operator of the tractor. This operator was the author and/or FPI employees. Testing of hydraulic vehicles has been done before at FPI, and therefore, the same precautions that are taken with operation of any hydraulic

vehicle was applied to this testing. Examples of safety precautions taken were built-in mechanical disc brakes, a spotter with clear eyesight and communication to the vehicle operator, ear protection and safety glasses, and similar safety items. The vehicle was operated on blocks during commissioning of the new VCU and while safety systems were tested.

Because this vehicle is intended to be a tool for FPI and MSOE students, it is not expected to be associated with any security concerns, except for the operator's key. The keys to operate this vehicle were available to students who are trained in how to operate and/or maintain this vehicle. The keys for the tractor are controlled by FPI staff members. This is standard FPI procedure.

Nearly the entire vehicle wiring harness was redone, along with several electrical sensors removed or replaced. The frame of the vehicle was found to be in much worse condition than initially thought. The engine of the vehicle was not able to run at full speed due to an unknown reason. These issues can be resolved with time, resources and attention by future MSOE student groups or clubs. For the purposes of this project, it did limit the type and amount of experimental testing that was able to be performed with the tractor.

The original steering sensor on the tractor was damaged and replaced with a similar sensor. This new sensor's electrical output was found to be inadequate once electrical power was applied and the sensor was tested. This resulted in unstable controls that used the steering sensor as an input. Therefore, any differential steering controls were removed from the control scheme that was downloaded onto the VCU. This issue requires a re-design consideration that was not initially part of the scope of this project.

Therefore, the tractor was not validated on the ground, and instead all tests were conducted with the tractor raised up on vehicle jacks.

This limitation means that a new simulation was run with the vehicle weight equal to zero pounds. Comparing this simulation to the no load condition of the tractor still provides excellent insight into the tractor's HST properties.

To collect data, a vehicle dashboard was created using a Raspberry Pi 3, touch screen, CANBus hat, and programmed in Python. This dashboard can receive and send information to the VCU and was programmed to log specific sensor and vehicle information for the purposes of troubleshooting and analysis. The VCU also comes with software from Husco which allows for the logging of CANBus data from the VCU. This software was used to record data as well as the newly constructed vehicle dashboard.

Many hours were spent troubleshooting the initial startup and commissioning of the tractor's electrical, mechanical and hydraulic systems. Once the HST's directional control valves were properly calibrated, a replication of the accelerator pedal input from the simulation could be performed. The data from this test are compared to the no load simulation of the tractor in the following section.

Experimental Results

There are a limited number of simulation values that can be directly verified by experimental testing, due to the limitation of sensor placement, cost, and feasibility. The physical signals that could be recorded during testing include the left and right HST side A pressure line and the left and right wheel speeds.

The engine speed could not be logged synchronously at this time due to the lack

of pulse input pins on the vehicle's VCU. A signal conditioner could be installed in the future to allow this signal to be recorded. For this test, the engine speed was observed on a digital tachometer by the vehicle operator during testing. The speed of the engine remained mostly constant during testing, due to the very low load on the engine. The engine speed was recorded to be 1910 RPMs. This constant engine value was used in the simulation for experimental validation.

Once experimental data were gathered, the effective damping factor was adjusted to 0.08 lbm/s based on the HST side A pressure measured during full speed steady state. The charge pump pressure was also adjusted from 100 psi to 500 psi, as this was the actual setting on the tractor. No other estimated parameters were changed in the simulation after comparing experimental results. Figure 20 shows the results of validation testing for the left side HST pressure.

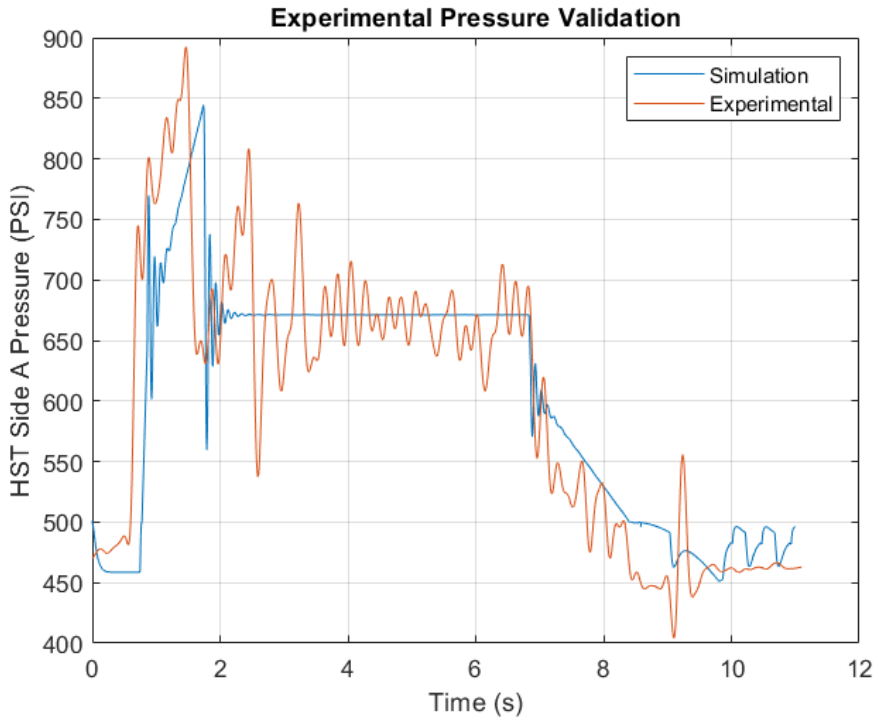

Figure 20: Left side HST Pressure During Experimental Validation Testing.

The general shape of the simulated pressure of the HST's side A can be seen to match the experimental data. The simulation is lacking the pressure ripples that occur in hydraulic systems due to individual pump and/or motor cylinder compressions. There are more complex ways to model the transmission lines that will result in the appearance of these pump and motor pressure ripples, which may be investigated in the future. The simulation's lack of higher speed pressure ripples will likely not cause any control issues in future closed loop control schemes. This is due to the fact that the controller does not consider pressure feedback to adjust pump displacement. One possible future use of the pressure values in the VCU could be to lower the pump's displacement in an engine stall condition. This control feature could be for protection of the engine and convenience of the operator. Figure 21 shows the results of validation testing for the wheel speed.

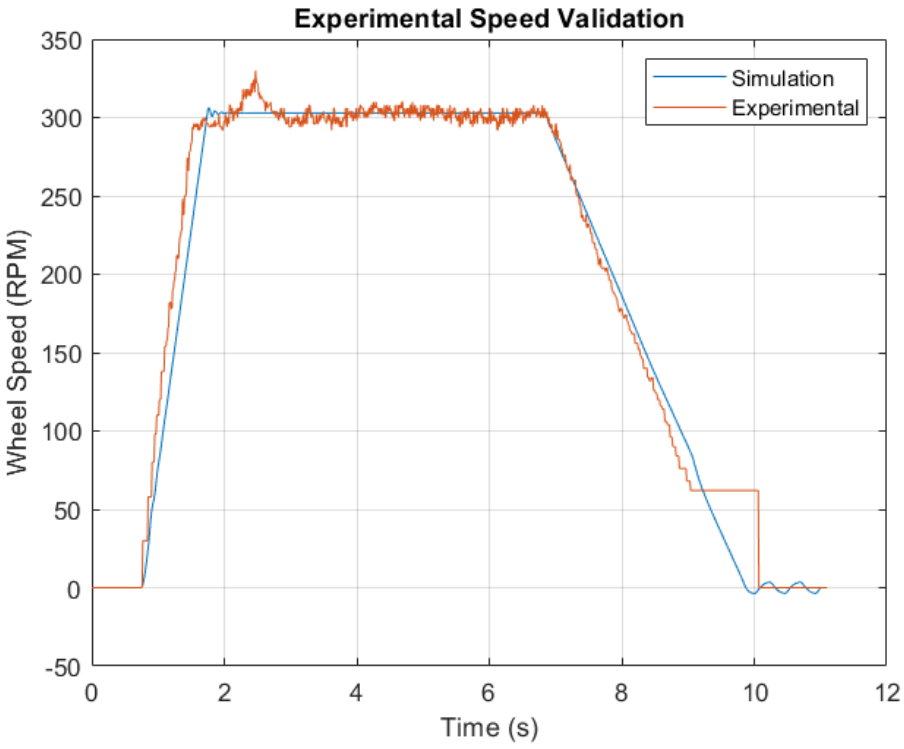

Figure 21: Left Side Wheel Speed During Experimental Validation Testing.

It can be seen in Figure 21 that the simulated wheel speed very closely tracks the experimental data. It was noticed during the testing that at second 2.5, the engine speed spiked for a short amount of time, as seen in Figure 21. There is an anomaly in the wheel speed value in the VCU that occurs when the wheel speed transitions from 50 rpm to 0 rpm. It is unknown why the controller interprets a constant value for about a second and then drops to 0 speed. There may be some type of signal conditioning that is occurring for the frequency input channel of the VCU that causes this unwanted behavior to occur. It is unknown if this behavior will affect low speed closed loop speed control in the future.

Conclusions and Recommendations

The Simulink model successfully conveys the power exchanges from the tractor's engine, through the HST, into the wheel, and finally into vehicle motion. When more torque is needed for more acceleration, the pressure in the transmission lines increase and torque increase is seen from the pump and the engine. This is what one would expect to see in a hydrostatic vehicle.

The results of the experimental testing show good agreement between the simulated output of model, and the tractor's actual wheel speed. The input of the model is the accelerator pedal, and the output of the model is the vehicle speed. Based on similar inputs in the model and real-world tests, the outputs for both scenarios are very similar. The HST model is ready to be used by future MSOE teams.

There is some future work that may be done after this project. This model does not account for negative engine torque loads. When braking, the ICE consumes energy

instead of providing it. In the real world, this would cause an engine overspeed. This aspect of the model could be improved.

This model also does not deal with pump or motor inefficiencies. There is leakage flow from each HST line to account for these pump and motor inefficiencies. Future work could include inefficiencies, both mechanical and volumetric that more closely resembles the actual workings of this tractor. This model has many areas that have been ignored or left blank in hopes that other projects will add more components. Those components include external loads, rolling resistance, engine speed sensor, engine lugging protection, steering sensor and steering control schemes.

A last area of future work would include the speed controls. This model uses open loop speed control. Using a closed loop control with speed feedback of the wheels would allow for better speed control of the tractor's wheels. An electronic and programmable dashboard was created for this project for future MSOE teams to use. This dashboard could allow for controller gains and other tunable variables to be easily changed while operating the vehicle. This dashboard also allows for data logs to be taken without the need for an external computer to be connected to the tractor. This should help reduce the risk of damage by not having a computer connected to a moving vehicle.

As of the publication of this paper, there is an MSOE undergraduate senior design team that will be utilizing this tractor, its new VCU, and the simulation produced by this capstone project. The senior design team will be electrifying the tractor by removing the ICE and installing an electric motor and battery pack. The senior design team will be building their project from the tools that were developed during this capstone project. This project was successful in providing a platform for future MSOE teams to use in their

academic projects.

References

[1] Johnson, J. 2010. "Understanding Hydrostatic Transmissions." *Hydraulics & Pneumatics.* [Internet, WWW]. *Available*: Available from the *Hydraulics & Pneumatics* website; ADDRESS: https://www.hydraulicspneumatics.com/technologies/hydraulic-pumps-motors/article/21885025/understanding-hydrostatic-transmissions

[2] Magnom News. 2018. "Hydrostatic Filtration for Main Loop/Circuit Component Protection." [Internet, WWW]. *Available:* Available from the *Magnom* website; ADDRESS: https://magnom.com/2018/06/hydrostatic-filtration-for-main-loop-circuit-component-protection

[3] McLaren, R. 2006. "Does Your Hydrostatically Propelled Vehicle Have Brakes?" *Fluid Power Safety Institute*. [Internet, WWW]. *Available:* Available from the *Fluid Power Safety Institute* website; ADDRESS: http://www.fluidpowersafety.com/fpsi_alert-30.html

[4] Nevala, K., Penttinen, J., and Saavalainen, P. 1998. "Developing of the Anti-Slip Control of Hydrostatic Power Transmission for Forest Tractor and Optimisation of the Power of Diesel Engine." *Proceedings of the 1998 5th International Workshop on Advanced Motion Control [AMC '98 COIMBRA],* pp.475-480. [Internet, WWW, Database]. *Available:* Available from the IEEE Xplore Database; ADDRESS: https://doi.org/10.1109/AMC.1998.743583

[5] Eaton. 2021. "HFX Programmable Controllers." [Internet, WWW]. *Available:* Available from the *Eaton* website; ADDRESS: https://www.eaton.com/ecm/groups/public/@pub/@eaton/@hyd/documents/content/pct_1126323.pdf. [Accessed: 31 October 2022].

[6] Tregue, C. 27 April 2021. “What Lidar Is and Why It’s Important for Autonomous Vehicle.” [Internet, WWW]. *Available*: Available on the *Autoweek* Website; ADDRESS: https://www.autoweek.com/news/a36190274/what-lidar-is/

[7] Wilson, W. E. 1950. *Positive Displacement Pumps and Fluid Motors.* New York: Pitman Publishing.

[8] Panwar, P. and Michael, P. 2018. "Empirical Modelling of Hydraulic Pumps and Motors." *International Journal of Hydromechatronics,* Vol. 21, No. 3, pp. 272-292. [Internet, WWW, PDF]. *Available:* Available from the ResearchGate site; ADDRESS: https://doi.org/10.1504/IJHM.2018.094880

[9] Egeland, O. and Gravdahl, J. 2002. *Modeling and Simulation for Automatic Control.* Trondheim, Norway: Marine Cybernetics.

[10] Nalbach, C., Ottman, Z., Otto, A., Rochefort, D., and Schmidt, P. 20 February 2017. “ASABE International 1/4 Scale -Tractor Student Design Competition.” ME 491 Senior Design Report, Mechanical Engineering Department, Milwaukee School of Engineering (MSOE), Milwaukee, WI.

[11] Watton, J. 2009. *Fundamentals of Fluid Power Control.* New York, NY: Cambridge University Press.

[12] Ogata, K. 2004. *System Dynamics.* Upper Saddle River, NJ: Pearson Prentice Hall.

[13] Dudek, G. and Jenkin, M. 2010. *Computational Principles of Mobile Robotics*. New York, NY: Cambridge University Press.

[14] Guzzella, L. and Onder, C. H. 2010. *Introduction to Modelling and Control of Internal Combustion Engine Systems.* Chennai, India: Scientific Publishing Services.

[15] Poclain. 2021. "PM10 Variable Displacement Pump Closed Loop Circuit." Poclain. [Internet, WWW, PDF]. *Available:* Available from the *Poclain* website: ADDRESS: https://hydraulicsonline.com/wp-content/uploads/2020/04/Poclaim-PM10.pdf. [Accessed 31 October 2022]

[16] Eaton. 2018. "Low Speed, High Torque Motors." [Internet, WWW, PDF]. *Available:* Available from the Eaton website; ADDRESS: https://www.eaton.com/ecm/groups/public/@pub/@eaton/@hyd/documents/content/pll_1323.pdf. [Accessed 31 10 2021].

[17] Merritt, H. E. 1967. *Hydraulic Control Systems.* New York: J Wiley & Sons.

[18] Manring, N. D. 2005. *Hydraulic Control System.* New York: J Wiley & Sons.

[19] Lennevi, J. 1995. *Hydrostatic Transmission Control*. Linköping, Sweden. UniTryck Linköping.

[20] Prasetiawan, E. A., Zhang, R. Alleyne, A. G. 1999. "Modeling and Control Design of a Powertrain Simulation Testbed for Earthmoving Vehicles." *American Society of Mechanical Engineers, The Fluid Power and Systems Technology Division (Publication) FPST*, Vol 6, pp. 139-146. [Internet, WWW]. *Available:* Available from *Scopus* website; ADDRESS: https://asmedigitalcollection.asme.org/IMECE/proceedings-abstract/IMECE99/139/1130189

[21] Jedrzykiewicz, Z., Pluta, J. and Stojek, J. 1998. "Application of the MATLAB - Simulink Packge in the Simulation Tests on Hydrostatic Systems." *Acta Montanistica Slovaca,* Vol. 3, No. 1, pp. 29-36. [Internet, WWW]. *Available:* Available from *ResearchGate* site; ADDRESS: https://www.researchgate.net/publication/26401963_Application_of_the_MATLAB_-_Simulink_package_in_the_simulation_tests_on_hydrostatic_systems

[22] Carlsson, E. 2006. *Modeling Hydrostatic Transmission.* Dissertation, Department of Electrical Engineering, Link¨opings Universitet. [Internet, WWW]. *Available:* Available from *DiVA* site; ADDRESS: http://liu.diva-portal.org/smash/record.jsf?pid=diva2%3A22028&dswid=8831

[23] Shevchenko, N. 2020. "An Introduction to Model-Based Systems Engineering (MBSE)." *Carnegie Mellon University SEI Blog.* [Internet, WWW]. *Available*: Available from the *Carnegie Mellon University SEI* website; ADDRESS: https://insights.sei.cmu.edu/blog/introduction-model-based-systems-engineering-mbse

[23] Williams, D. Winter 2021. “ME 5980: Mechanical System Simulation.” Graduate course presented at the Milwaukee School Of Engineering. Milwaukee, Wisconsin.

Appendix A: Simulink Sub-Models

Appendix A features the remaining Simulink sub-models not seen in the paper's previous sections for this project. The sub-models include charge pump, check valve, relief valve, flushing valve, pump, motor, motor flow, motor torque, wheel [24]. The sub-models also include the vehicle control, safety mode, load, and vehicle kinematics.

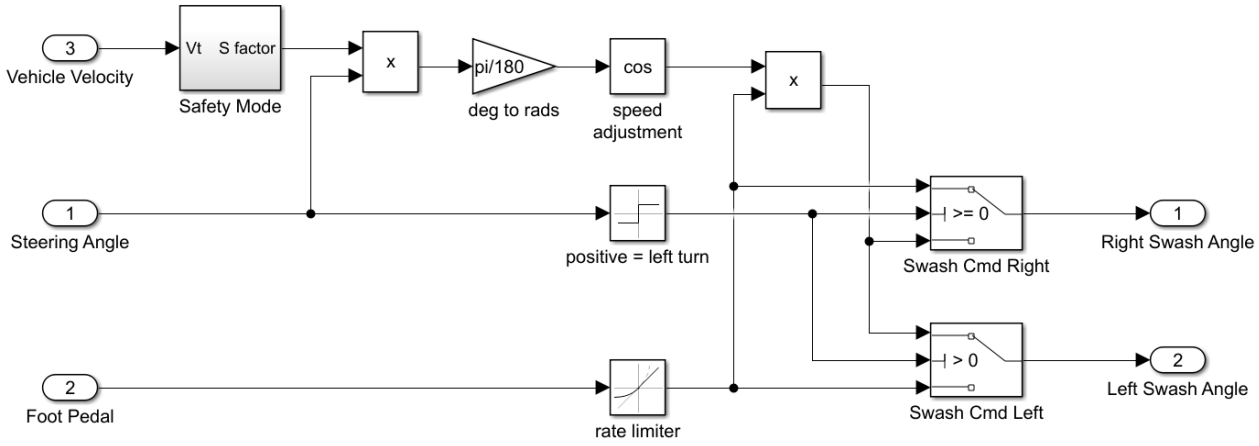

Figure A-1: Vehicle Control Sub-Model.

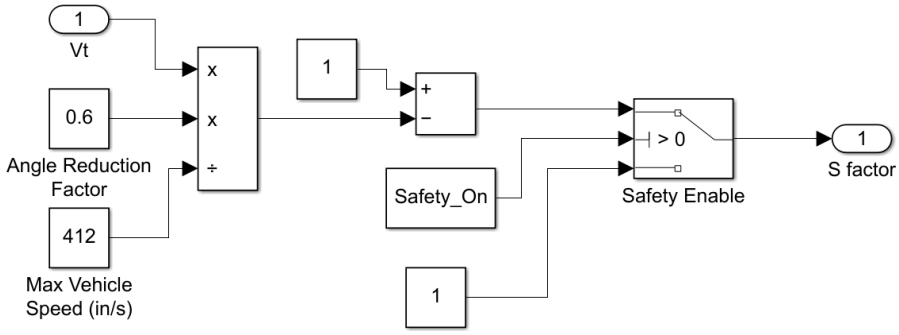

Figure A-2: Safety Mode Sub-Model.

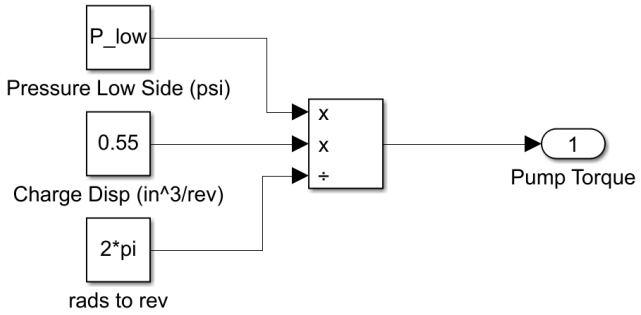

Figure A-3: Charge Pump Sub-Model

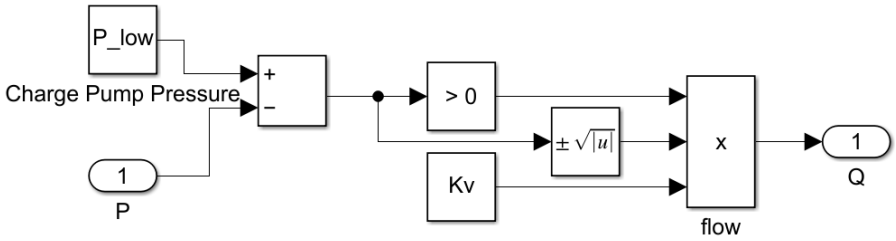

Figure A-4: Check Valve Sub-Model.

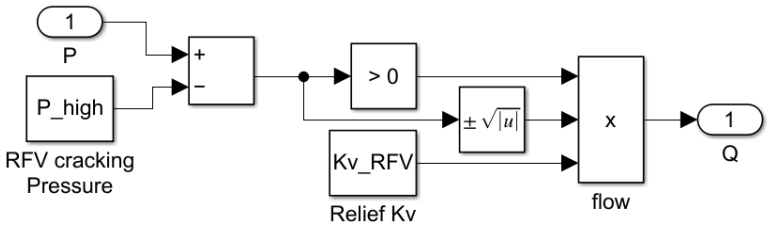

Figure A-5: Relief Valve Sub-Model.

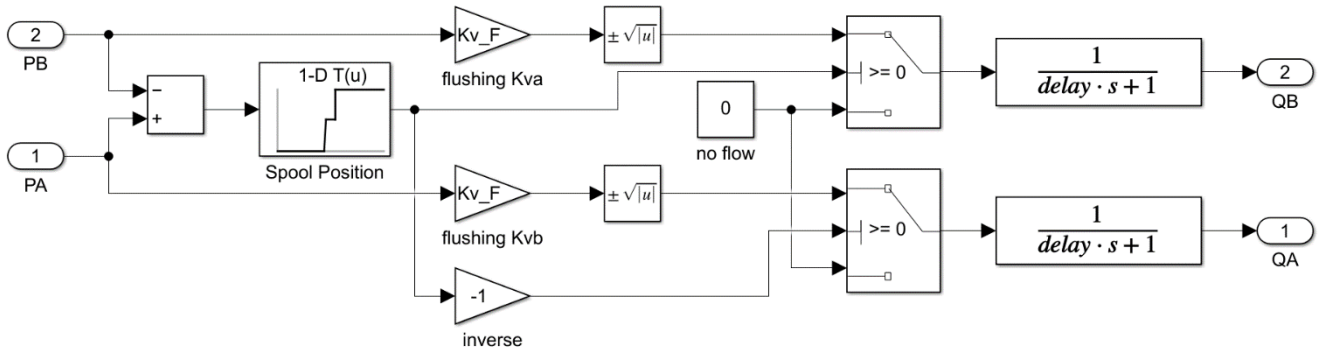

Figure A-6: Flushing Valve Sub-Model.

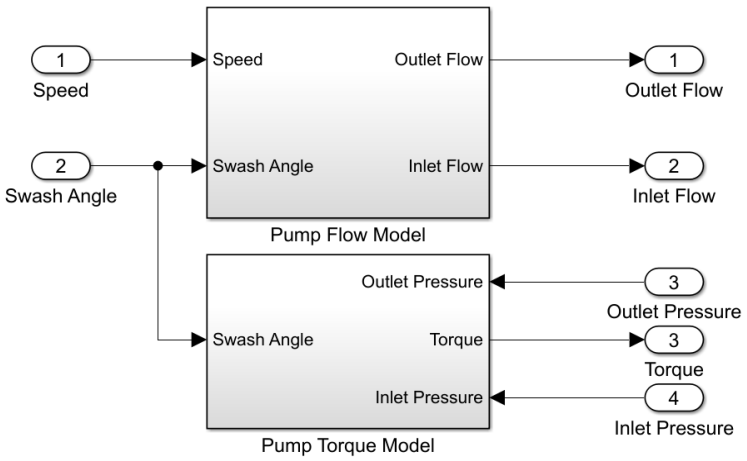

Figure A-7: Pump Sub-Model.

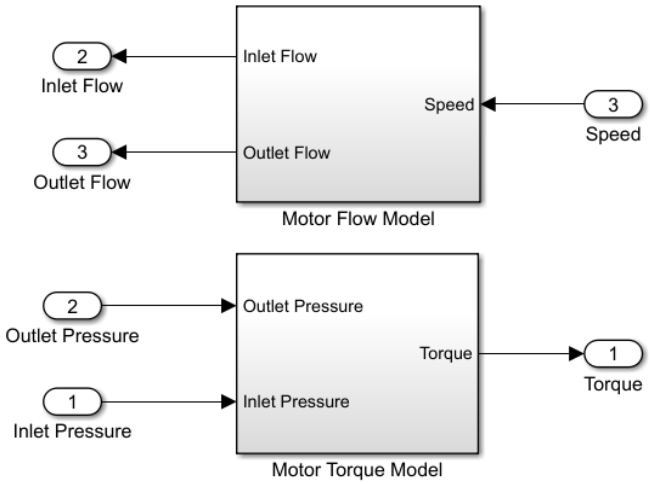

Figure A-8: Motor Sub-Model.

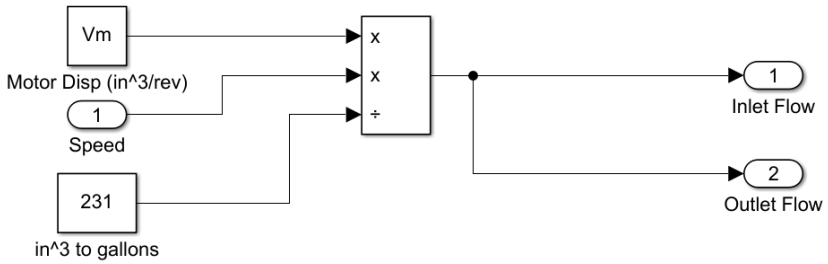

Figure A-9: Motor Flow Sub-Model.

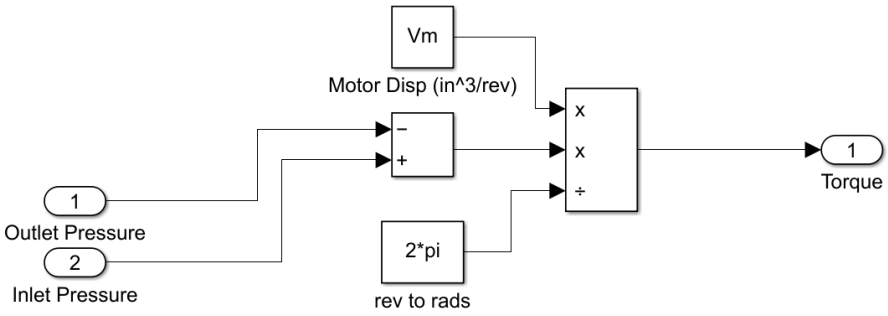

Figure A-10: Motor Torque Sub-Model.

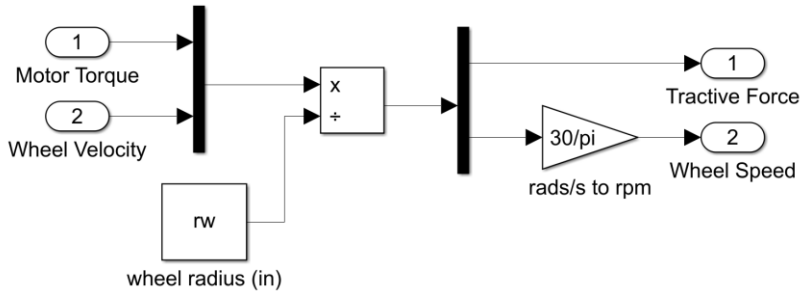

Figure A-11: Wheel Sub-Model.

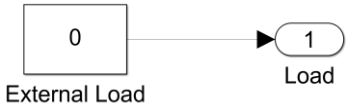

Figure A-12: Load Sub-Model.

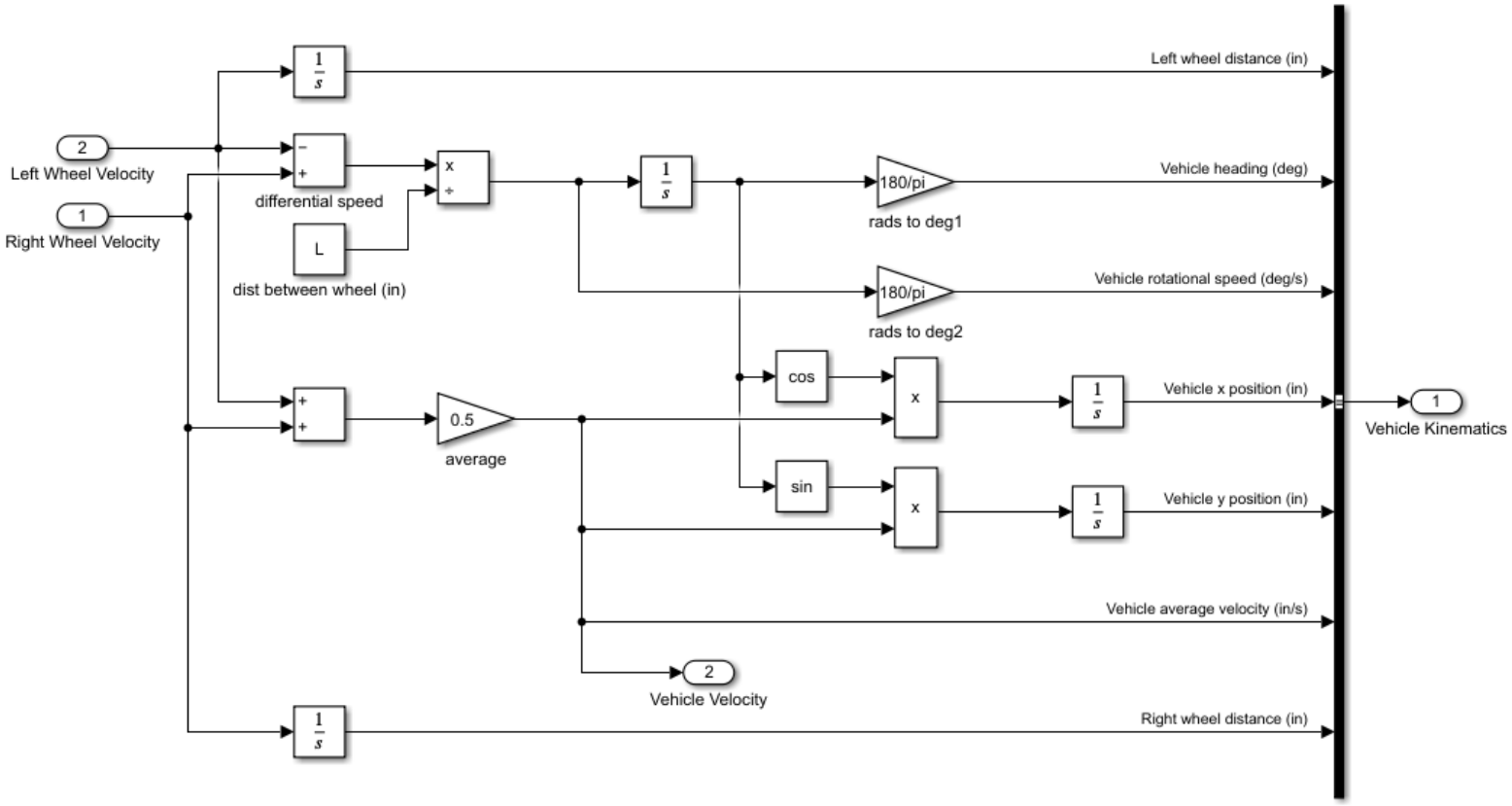

Figure A-13: Vehicle Kinematics Sub-Model.

Engineering

Capstone Report Approval Form

Master of Science in Engineering – MSE

Milwaukee School Of Engineering

This capstone report, titled “Model and Control of Tractor with Dual Independent Rear Wheel Hydrostatic Transmissions,” submitted by the student Lucas Garcia, has been approved by the following committee:

Faculty Advisor: _____ Date: _____

Dr. Daniel Williams, Ph.D.

Faculty Member: _____ Date: _____

Dr. Subha Kumpaty, Ph.D.

Faculty Member: _____ Date: _____

Professor Gary Shimek, M.L.I.S.